AFRL-ML-WP-TP-2007-532

PHOTOEXCITED-CARRIER-INDUCED REFRACTIVE-INDEX CHANGE IN SMALL BAND-GAP SEMICONDUCTORS (PREPRINT)

Z.G. Yu, S. Krishnamurthy, and Shekhar Guha

Hardened Materials Branch
Survivability and Sensor Materials Division

AUGUST 2006

STINFO COPY

AIR FORCE RESEARCH LABORATORY
MATERIALS AND MANUFACTURING DIRECTORATE
WRIGHT-PATTERSON AIR FORCE BASE, OH 45433-7750
AIR FORCE MATERIEL COMMAND
UNITED STATES AIR FORCE

NOTICE AND SIGNATURE PAGE

This report was cleared for public release by the Air Force Research Laboratory Wright Site (AFRL/WS) Public Affairs Office and is available to the general public, including foreign nationals. Copies may be obtained from the Defense Technical Information Center (DTIC) (http://www.dtic.mil).

AFRL-ML-WP-TP-2007-532 HAS BEEN REVIEWED AND IS APPROVED FOR PUBLICATION IN ACCORDANCE WITH ASSIGNED DISTRIBUTION STATEMENT.

*//Signature//   //Signature//

SHEKHAR GUHA, Ph.D.   MARK S. FORTE, Acting Chief
Agile IR Limiters   Hardened Materials Branch
Exploratory Development   Survivability and Sensor Materials Division
Hardened Materials Branch

//Signature//

TIM J. SCHUMACHER, Chief
Survivability and Sensor Materials Division

REPORT DOCUMENTATION PAGE

Form Approved
OMB No. 0704-0188

1. REPORT DATE *(DD-MM-YY)*	2. REPORT TYPE	3. DATES COVERED *(From - To)*
August 2006	Journal Article Preprint	

4. TITLE AND SUBTITLE	5a. CONTRACT NUMBER
PHOTOEXCITED-CARRIER-INDUCED REFRACTIVE-INDEX CHANGE IN SMALL BAND-GAP SEMICONDUCTORS (PREPRINT)	In-house
	5b. GRANT NUMBER
	5c. PROGRAM ELEMENT NUMBER 62102F

6. AUTHOR(S)	5d. PROJECT NUMBER 4348
Z.G. Yu and S. Krishnamurthy (SRI International) Shekhar Guha (AFRL/MLPJ)	5e. TASK NUMBER RG
	5f. WORK UNIT NUMBER M08R1000

7. PERFORMING ORGANIZATION NAME(S) AND ADDRESS(ES)		8. PERFORMING ORGANIZATION REPORT NUMBER
SRI International 332 Waverly Street Menlo Park, CA 94025	Hardened Materials Branch (AFRL/MLPJ) Survivability and Sensor Materials Division Materials and Manufacturing Directorate Wright-Patterson Air Force Base, OH 45433-7750 Air Force Materiel Command United States Air Force	AFRL-ML-WP-TP-2007-532

9. SPONSORING/MONITORING AGENCY NAME(S) AND ADDRESS(ES)	10. SPONSORING/MONITORING AGENCY ACRONYM(S)
Air Force Research Laboratory Materials and Manufacturing Directorate Wright-Patterson Air Force Base, OH 45433-7750 Air Force Materiel Command United States Air Force	AFRL/MLPJ
	11. SPONSORING/MONITORING AGENCY REPORT NUMBER(S) AFRL-ML-WP-TP-2007-532

12. DISTRIBUTION/AVAILABILITY STATEMENT
Approved for public release; distribution unlimited.

13. SUPPLEMENTARY NOTES
Journal article submitted to the Journal of the Optical Society of America. The U.S. Government is joint author of this work and has the right to use, modify, reproduce, release, perform, display, or disclose the work. PAO Case Number: AFRL/WS 06-2028, 21 Aug 2006.

14. ABSTRACT
Using accurate band structures of InAs, InSb, and two $Hg_{1-x}Cd_xTe$ alloys, we calculate the change in refractive index caused by the photoexcited electrons and holes. The effect of both free-carrier absorption (FCA) and one-photon absorption are considered. We find that the change in refractive index varies nonlinearly with the density of photoexcited carriers and that the generally neglected FCA contribution is significant in InAs, owing to its weak spin-orbit coupling.

15. SUBJECT TERMS
Refractive Index, Photoexcited Carriers, One-Photon Absorption, Free-Carrier Absorption

16. SECURITY CLASSIFICATION OF:			17. LIMITATION OF ABSTRACT:	18. NUMBER OF PAGES	19a. NAME OF RESPONSIBLE PERSON (Monitor)
a. REPORT Unclassified	b. ABSTRACT Unclassified	c. THIS PAGE Unclassified	SAR	18	Shekhar Guha 19b. TELEPHONE NUMBER *(Include Area Code)* N/A

Standard Form 298 (Rev. 8-98)
Prescribed by ANSI Std. Z39-18

Photoexcited-carrier-induced refractive-index change in small band-gap semiconductors

Z. G. Yu and S. Krishnamurthy
SRI International, Menlo Park, CA 94025

Shekhar Guha
Wright-Patterson AFB, Dayton, Ohio 45433

Abstract

Using accurate band structures of InAs, InSb, and two $Hg_{1-x}Cd_xTe$ alloys, we calculate the change in refractive index caused by the photoexcited electrons and holes. The effect of both free-carrier absorption (FCA) and one-photon absorption are considered. We find that the change in refractive index varies nonlinearly with the density of photoexcited carriers and that the generally neglected FCA contribution is significant in InAs, owing to its weak spin-orbit coupling.

Key words: refractive index, photoexcited carriers, one-photon absorption, and free-carrier absorption

I. Introduction

Semiconductor materials such as InSb, InAs and HgCdTe are used in opto-electronic applications including quantum cascade lasers, terahertz generation, and saturable absorbers [1-2]. These applications involve generation of high levels of charge carriers that render it important to understand the effect of photoexcited carriers on the material optical properties. In addition, high-intensity light propagation in semiconductors can be strongly affected by the generation of a high density of photoexcited carriers. The incident light creates electron-hole pairs, some of which recombine through a variety of mechanisms including the Auger, radiative, and Shockley-Read-Hall (SRH) processes. Not all electron-hole pairs will recombine before the entry of the next stream of photons, and the excess excited carriers will alter the photon absorption both above and below the fundamental gap. As a result, the refractive index changes from its value at equilibrium. Although there are a number of studies to accurately calculate the absorption and carrier relaxation in semiconductors, only simplified models that use effective mass bandstructures, the Boltzmann distribution for the carriers, and one-photon absorption (OPA) across the band gap are currently being employed in the evaluation of refractive index changes [3-7]. These calculations predict that the change in refractive index varies linearly with the carrier density and increases with lattice temperature. The contribution from free carrier absorption (FCA) is only considered within the Drude approximation [8].

In this paper, we use full band structures and Fermi-Dirac (FD) statistics for photo-excited carriers to systematically calculate the change in refractive index arising from both OPA and FCA in four direct band-gap semiconductors: two having band gaps less than 0.21 eV (InSb and $Hg_{0.762}Cd_{0.238}Te$) and two having a band gap approximately 0.35 eV (InAs and $Hg_{0.656}Cd_{0.344}Te$). The results from this accurate calculation differ from the existing results not only in the magnitude, but also in the trend. The calculated change in refractive index (a) varies highly nonlinearly with the excess carrier density in the two smaller band gap materials but almost linearly in the two larger band gap materials, (b) has a considerable contribution from FCA in InAs, where the spin-orbit (SO) splitting is small.

2

II. Formalism:

The photoexcited carriers in the conduction and valence bands modify the absorption spectrum, which results in a change in the refractive index through the Kramers-Kronig relation between the real part of the refractive index, n_1, and the absorption coefficient, $\alpha(\omega)$,

$$n_1(\omega) - 1 = \frac{c}{\pi} P \int_0^\infty \frac{\alpha(\omega')d\omega'}{\omega'^2 - \omega^2} \qquad (1)$$

where c is the speed of light, ω is the angular frequency, and P indicates principle value of the integral. The refractive index change, Δn_1, arising from the excess carriers, can be calculated from [9]

$$\Delta n_1(\omega) = \frac{c}{\pi} P \int_0^\infty \frac{\alpha(\omega',\Delta N) - \alpha(\omega',0)}{\omega'^2 - \omega^2} d\omega' \qquad (2)$$

where $\alpha(\omega',\Delta N)$ and $\alpha(\omega',0)$ are the absorption coefficients at angular frequency of ω' in the presence of photoexcited electron-hole pairs with the density of ΔN and in equilibrium, respectively.

The absorption coefficient is related to the imaginary part of the dielectric function, $\varepsilon_2(\omega)$, via $\alpha(\omega) = \frac{\omega \varepsilon_2(\omega)}{n_1(\omega)c}$. For a small change in refractive index, $n_1(\omega)$ in this relation can be replaced by $n^0_1(\omega)$, which is the refractive index for the system in equilibrium. The absorption change can then be written in terms of the change in the dielectric function,

$$\alpha(\omega,\Delta N) - \alpha_0(\omega) = \frac{\omega}{n^0_1(\omega)c} \left[\varepsilon_2(\omega,\Delta N) - \varepsilon_2(\omega,0) \right] \qquad (3)$$

where $\varepsilon_2(\omega,0)$ and $\varepsilon_2(\omega,\Delta N)$ are the imaginary part of the dielectric function for the system in equilibrium and in the presence of additional electron-hole pairs with density ΔN, respectively.

Among many absorption processes the FCA and OPA are most sensitive to the carrier occupation in a small band-gap material. The OPA excites an electron from the valence band into the conduction band when the photon has energy greater than the band gap. To achieve this

3

interband transition, the initial state in the valence band must be occupied and the final state in the conduction band must be vacant. The photoexcited carriers change the occupation in both conduction and valence bands when compared to the system in equilibrium and thus modify the OPA. When the energy of a photon is not large enough to enable the valence band to conduction band transitions, the carriers can still absorb the photon through intra-band transitions (with the help of phonons) and inter-valence band transitions, commonly known as FCA. Since both these processes are proportional to the number of carriers, the photoexcited carriers will modify the FCA spectrum as well.

We calculate the change in dielectric function arising from the OPA and FCA by electrons and holes using accurate band structures and wave functions from a long-range tight-binding Hamiltonian [10]. The OPA contribution to $\varepsilon_2(\omega, \Delta N)$ can be calculated from

$$\varepsilon_2(\omega, \Delta N) = \frac{4\pi^2 e^2}{3m_0^2 \omega^2} \sum_{nm\mathbf{k}} |\mathbf{p}_{nm}(\mathbf{k})|^2 f(E_{m\mathbf{k}})[1 - f(E_{n\mathbf{k}})]\delta(E_{n\mathbf{k}} - E_{m\mathbf{k}} - \hbar\omega), \qquad (4)$$

where e is the electron charge, m_0 is the free-electron mass, n and m are the conduction and valence band indices, respectively, $E_{n\mathbf{k}}$ and $E_{m\mathbf{k}}$ are the corresponding band energies, and p_{nm} are the interband momentum matrix elements. f is the charge carrier distribution function,

$$\begin{aligned} f(E_{m\mathbf{k}}) &= [1 + e^{\beta(E_{m\mathbf{k}} - \mu_h)}]^{-1} \\ f(E_{n\mathbf{k}}) &= [1 + e^{\beta(E_{n\mathbf{k}} - \mu_e)}]^{-1} \end{aligned} \qquad (5)$$

where μ_e and μ_h are the Fermi levels for electrons and holes respectively, which are determined from the density of photoexcited electron-hole pairs, ΔN. When $\Delta N = 0$, μ_e and μ_h are equal.

The FCA contribution to $\varepsilon_2(\omega, \Delta N)$ includes two parts. The first is that electrons in the conduction bands (or holes in the valence bands) absorb an LO photon and make a transition to a higher-energy state within the same band. This contribution is calculated from

$$\varepsilon_2(\omega, \Delta N) = \frac{8\pi^3 e^4 \omega_{LO}}{\hbar\omega^3 m_0^2 V}\left(\frac{1}{\kappa_\infty} - \frac{1}{\kappa_0}\right)\sum_{n\mathbf{k}} f(E_{n\mathbf{k}})R_{n\mathbf{k}} \qquad (6)$$

$$R_{n\mathbf{k}} = \sum_{n\mathbf{q}\pm}\left(N_{LO} + \frac{1}{2} \mp \frac{1}{2}\right)\left|\left\langle n\mathbf{k} \pm \mathbf{q}\left|\frac{e^{i\mathbf{q}\cdot\mathbf{r}}}{q}\right|n\mathbf{k}\right\rangle\left(\left\langle n\mathbf{k}\left|\sum_j \mathbf{e}_j \cdot \mathbf{p}\right|n\mathbf{k}\right\rangle - \left\langle n\mathbf{k} + \mathbf{q}\left|\sum_j \mathbf{e}_j \cdot \mathbf{p}\right|n\mathbf{k} + \mathbf{q}\right\rangle\right)\right| \quad (7)$$

where n is the band index, $\hbar\omega_{LO}$ is the LO phonon energy, and N_{LO} is the number of LO phonons that can be obtained from the Bose-Einstein distribution function. We have used the Fröhlich Hamiltonian to describe the coupling between the electrons and LO-phonons. The

4

second arises from photon absorption by holes, without a phonon, making a direct transition between the heavy-hole and light-hole valence bands. This contribution is calculated from

$$\varepsilon_2(\omega, \Delta N) = \frac{4\pi^2 e^2}{3m_0^2 \omega^2} \sum_{mm'\mathbf{k}} |\mathbf{p}_{mm'}(\mathbf{k})|^2 f(E_{m\mathbf{k}})[1 - f(E_{m'\mathbf{k}})]\delta(E_{m'\mathbf{k}} - E_{m\mathbf{k}} - \hbar\omega),$$ (8)

where m and m' are valence-band indices.

It should be noted from Eqs. (2) and (3) that the dielectric function needs to be computed over a very large frequency range even if Δn_1 is evaluated only near the band edge frequencies. In addition, a careful numerical evaluation of the integral in Eq. (2) is required because of the singularity in the integrand.

III. Results and discussions

To test the accuracy of the band structures and dipole matrix elements used in our calculations, we have computed the OPA coefficients in InSb and InAs and found those to be in excellent agreement with the measured values. The dielectric function and the change in the refractive index are then calculated for the two materials with band gap E_g of 0.35 eV -- InAs and $Hg_{0.656}Cd_{0.344}Te$, and the two smaller band-gap materials—InSb (E_g=0.173 eV) and $Hg_{0.762}Cd_{0.238}Te$ (E_g=0.206 eV). The spectra of $n^0{}_1(\omega)$ used in our calculations are from the literature [11-14].

Figure 1 shows the calculated change in refractive index as a function of wavelength due to the FCA and OPA in InSb at two densities of photoexcited electron-hole pairs --- $\Delta N=10^{16}$ and 10^{17} cm^{-3}. We see that the FCA contribution depends weakly on the wavelength. However, the OPA contribution shows a steep change near the band gap. This variation can be easily understood from Eq. (2). In the presence of photoexcited carriers, the band edge states are filled and the joint density of states of electrons and holes available for absorption decreases and the OPA is reduced. Thus the numerator of the integrand in Eq. (2) is either zero (for $\omega' < \omega_g$) or negative (for $\omega' > \omega_g$) with ω_g being the band gap frequency. When the frequency ω crosses ω_g, the denominator of the integrand changes sign and, consequently, $\Delta n_1(\omega)$ changes sign.

The calculated value of Δn_1 at λ =9.5 μm is shown in Fig. 2 as a function of photoexcited carrier density in InSb and $Hg_{0.762}Cd_{0.238}Te$. We see that in both materials the OPA contribution dominates over the FCA contribution to the Δn_1. Interestingly, the FCA contribution is positive, which is opposite of the OPA contribution at this wavelength. Similarly calculated results at λ

=4.8 μm for the larger band-gap materials — InAs and $Hg_{0.656}Cd_{0.344}Te$ — are plotted in Fig. 3. In this case, both FCA and OPA reduce the refractive index. Although both materials have the same band gap, in the HgCdTe alloy the dominant contribution is from the OPA, whereas in InAs both FCA and OPA have comparable contributions. To understand the different level of contribution of FCA to the refractive-index change, we plot the FCA cross section σ, as a function of wavelength in Fig. 4 for these two materials. The numerator of the integrand in Eq. (2) for the FCA process is proportional to this cross section and the FCA contribution to Δn_1 at a photon wavelength λ is roughly proportional to the difference in the areas below and above that λ in Fig. 4   We see that the absorption for wavelengths below λ =4.8 μm is negligible in InAs, but is significant in the HgCdTe alloy. Owing to a larger cancellation, the FCA contribution is smaller in the HgCdTe alloy. We explore further to understand the origin of the difference in the absorption spectrum of Fig. 4. In our calculations we found that most of the FCA arises from the transitions of holes from the heavy-hole to light-hole bands. Hence the different FCA spectra can be understood from the valance band structures in the two materials. We plot in Fig. 5 the energy difference between the heavy-hole and the light-hole valence bands as a function of wave vector **k** in symmetry directions for InAs and $Hg_{0.656}Cd_{0.344}Te$. In both cases the energy difference increases rapidly at small values of **k,** but saturates at 0.25 eV as the wave vector increases further in InAs. This small saturation value can be attributed to the weak SO coupling (0.38 eV) in InAs, which repels the light-hole valence band closer to the heavy-hole valence band. Absorption of photon with a larger energy than this saturation value is not possible. In the HgCdTe alloy, however, a larger SO coupling (0.95 eV) allows the light hole band to move farther away from the heavy-hole band, resulting in absorption at shorter wavelengths. Hence the relative contribution from OPA and FCA depend critically on the subtle details of the band structures.

The sum of the FCA and OPA induced change in refractive index, calculated at 4.8 μm for the large gap materials and at 9.5 μm for the small gap materials, is shown in Fig. 6 as a function of the density of photoexcited electron-hole pairs. Clearly the variation is nonlinear for the two smaller band-gap materials. An accurate fit to the total change indicated that variation is nonlinear even for the larger band-gap materials. Excellent fits to all four materials are obtained

by using a functional form $\Delta n_1 = a(1 - e^{-b\Delta N})$. Only for small ΔN ($< 10^{16}$ cm^{-3}) does the refractive index change linearly with ΔN. The fitted values of a and b are given in Table I.

It is interesting to estimate the effect of temperature on the OPA induced change in the refractive index. In our calculation with FD statistics and full band structures, the excess carrier induced change in OPA is nearly temperature independent. However, for example, the band gap in InSb changes from 0.173 eV at 300K to 0.234 eV at 77K. Since the contribution arising from OPA is nonzero only when $\omega' > \omega_g$, the denominator of the integrand in Eq. (2) is larger at T=77 K than at 300K, resulting in smaller change in the index. This conclusion is in contradiction with the previous studies [5,6], which used simplified band structures and Boltzmann distribution.

IV. Conclusions

In conclusion, we have calculated the change in refractive index arising from both the OPA and the FCA using full band structures for four materials, InSb, Hg$_{0.762}$Cd$_{0.238}$Te, InAs, and Hg$_{0.656}$Cd$_{0.344}$Te. We focus on the refractive-index change at λ=9.5 μm for the first two materials that have band gaps less than 0.21 eV and at λ=4.8 μm for the last two materials that have a band gap of 0.35 eV. The calculations show that the FCA contribution is not negligible and is comparable to the OPA contribution in InAs that has a small SO splitting. The calculated dependence of the change in refractive index on the density of photoexcited electron-hole pairs is strongly nonlinear in InSb and Hg$_{0.762}$Cd$_{0.238}$Te and moderately nonlinear in InAs and Hg$_{0.656}$Cd$_{0.344}$Te. Furthermore, the change in refractive index for InSb due to the OPA is smaller at lower temperatures than at room temperature because of a larger band gap at low temperatures.

References

1. W. S. Pelouch and L. A. Schlie, "Ultrafast carrier dynamics and saturable absorption in HgCdTe", Appl. Phys. Lett. **68**, 1389-1391 (1996).

2. S. Kono, P. Gu, M. Tani, and K. Sakai, "Temperature dependence of terahertz radiation from n-type InSb and n-type InAs surfaces", Appl. Phys. B **71**, 901-904 (2000).

3. For a review see, D.M. Kovsh, S. Yong, D.J. Hagan, and E. Van Stryland, "Nonlinear Optical Liquid for Power Limiting", SPIE **3472**, 163-177 (1998).

4. D.H. Auston, S. McAffee, C.V. Shank, E.P. Ippen, and O. Teschke, "Picosecond spectroscopy of semiconductors", Solid State Electron. **21**, 147-150 (1978).

5. D. A. B. Miller, C. T. Seaton, M. E. Prise, and S. D. Smith, "Band-gap-resonant nonlinear refraction in III-V semiconductors", Phys. Rev. Lett. **47**, 197-200 (1981).

6. E. W. van Stryland, Y.Y. Wu, D.J. Hagan, M.J. Soileau, K. Mansour, "Optical limiting with semiconductors", J. Opt. Soc. Am. **5**, 1980-1989 (1988).

7. P. P. Paskov and K. R. Koynov, "A theoretical analysis of absorption and refractive index changes in optically excited $In_{1-x}Ga_xSb$", Semicond. Sci. Technol. **9**, 1584-1590 (1994).

8. P. Paskov, "Refractive indices of InSb, InAs, GaSb, InAsSb and InGaSb: Effects of free carriers", J. Appl. Phys. **81**, 1890 (1997).

9. J. I. Pankove, *Optical Processes in Semiconductors* (Dover, New York, 1975), pp 90.

10. A.B. Chen and A. Sher, *Semiconductor Alloys* (Plenum, 1995), Ch. 5.

11. Z. Kucera, "Dispersion of the refractive index of $Hg_{1-x}Cd_xTe$", Phys. Status Solidi A, **100**, 659-665 (1987).

12. S. Rolland, "Dielectric constant and refractive index of HgCdTe" in *Properties of Narrow Gap Cadmium-Based Compounds*, P. Capper, ed (INSPEC, IEE, London, 1994). Pp 80-85.

13. E.D. Palik and R.T. Holm, "Indium Arsenide" in *Handbook of Optical Constants of Solids*, D. Palik, ed (Academic, San Diego, 1998) pp 479-489.

14. R.T. Holm, "Indium Antimonide" in *Handbook of Optical Constants of Solids*, D. Palik, ed (Academic, San Diego, 1998) pp 490-502.

Table 1: Fit parameters to obtain the calculated change in refractive index at 300K

Parameters	InAs	Hg$_{1-x}$Cd$_x$Te (x=0.344)	InSb	Hg$_{1-x}$Cd$_x$Te (x=0.238)
a	0.13067	0.14536	0.077854	0.12091
b	8.1952e-19	7.079e-19	2.9875e-18	1.6804e-18

Figure Captions:

Figure 1: Refractive-index change due to the FCA and OPA as a function of the photon wavelength in InSb with $\Delta N = 10^{16}$ and 10^{17} cm^{-3} at room temperature.

Figure 2: Refractive-index change at $\lambda = 9.5$ μm due to the FCA and OPA as a function of ΔN in InSb and $Hg_{0.762}Cd_{0.238}Te$ at room temperature.

Figure 3: Refractive-index change at $\lambda = 4.8$ μm due to the FCA and OPA as a function of ΔN in InAs and $Hg_{0.656}Cd_{0.344}Te$ at room temperature.

Figure 4: Cross section of the FCA σ as a function of the photon wavelength in InAs and $Hg_{0.656}Cd_{0.344}Te$ at room temperature.

Figure 5: Energy difference between the heave-hole and light-hole valence bands as a function of wave vector for InAs and $Hg_{0.656}Cd_{0.344}Te$ at room temperature.

Figure 6: Total change in the refractive index Δn_l at $\lambda = 4.8$ μm for InSb and $Hg_{0.762}Cd_{0.238}Te$ and at $\lambda = 9.5$ μm for InAs and $Hg_{0.656}Cd_{0.344}Te$ as a function of ΔN at room temperature.

Figure 1 Yu et al

Δn

FCA

FCA

OPA

OPA

InSb: 300 K
10^{17} cm^{-3} (solid)
10^{16} cm^{-3} (Dashed)

0.02
0.01
0.00
-0.01
-0.02
-0.03
-0.04
-0.05
-0.06

2   4   6   8   10   12

Wavelength [μm]

Figure 2 Yu et al

Δn

FCA

FCA

OPA

OPA

λ = 9.5μm
InSb
HCT-238

0.02
0.00
-0.02
-0.04
-0.06
-0.08
-0.10
-0.12

0.0   0.2   0.4   0.6   0.8   1.0x10^{18}

ΔN [cm^{-3}]

Figure 3 Yu et al

Δn

FCA

FCA

OPA

OPA

λ = 4.8 μm
InAs
HCT-344

0.00
-0.01
-0.02
-0.03
-0.04
-0.05
-0.06
-0.07

0.0   0.2   0.4   0.6   0.8   1.0x10^{18}

ΔN [cm^{-3}]

Figure 4 Yu et al

σ [10^{-16}cm^2]

InAs

HCT-344

12
10
8
6
4
2
0

0   10   20   30   40   50

λ [μm]

11
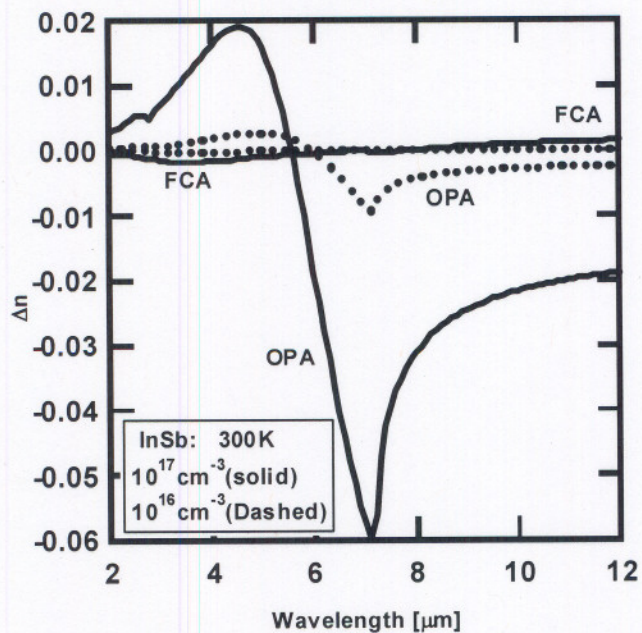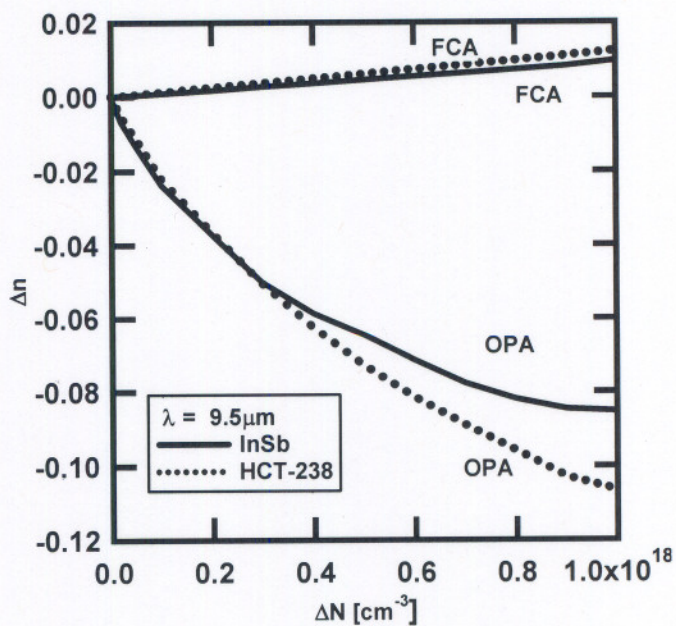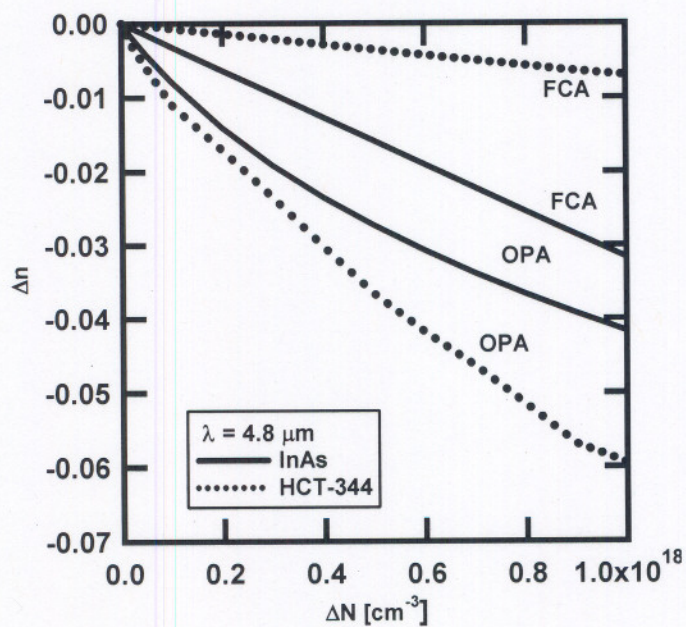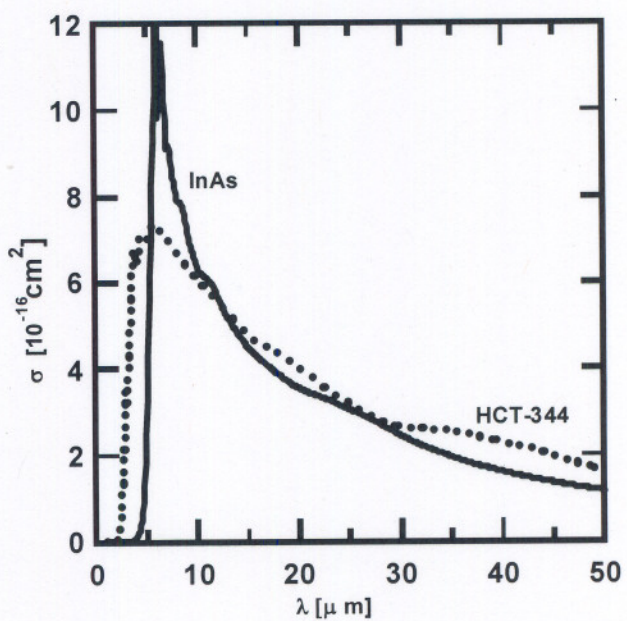
Figure 5 Yu et al   **Figure 6 Yu et al**